Multiwavelength Spectral Studies Of Fermi-LAT Blazars

Authors: Manasvita Joshi, A. Marscher, S. Jorstad (Boston U.), Markus Boettcher (Ohio U.), I. Agudo (Boston U. & IAA), V. Larionov (St. Petersburg State U.), M. Aller (U. Michigan), M. Gurwell (SAO), A.Lahteenmaki (Metsahovi Radio Obs.)

We present multiwavelength spectral analyses of OJ287 and 3C 279, using time-dependent, multi-slice leptonic jet model for blazars, with radiation feedback, in the internal shock scenario. We discuss the role of intrinsic parameters and interplay of synchrotron and inverse Compton radiation processes responsible for producing the resultant SEDs.

Abstract

We present multiwavelength spectral analyses of two Fermi-LAT blazars, OJ 287 and 3C 279, that are part of the Boston University multiwaveband polarization monitoring program. The data have been compiled from observations with Fermi, RXTE, the VLBA, and various ground-based optical and radio telescopes. We simulate the dynamic spectral energy distributions (SEDs) within the framework of a multi-slice, time-dependent leptonic jet model for blazars, with radiation feedback, in the internal shock scenario. We use the physical jet parameters obtained from the VLBA monitoring to guide our modeling efforts. We discuss the role of intrinsic parameters and the interplay between synchrotron and inverse Compton radiation processes responsible for producing the resultant SEDs.

Motivation

Blazar jets are highly violent in nature and are dominated by ultrarelativistic particles. The SED of blazars consists of two spectral bumps. The low-energy component is due to synchrotron radiation emanating from relativistic particles, and the high-energy component (for leptonic jet model) is a result of Compton upscattering of the seed photon field by ultrarelativistic particles [1]. The mode of acceleration of plasma electrons (and positrons) to highly relativistic energies and its location in the jet is still not completely understood. One way to comprehend the physics of particle acceleration is the internal shock model, in which the central engine (black hole + accretion disk) spews out shells of plasma with different velocity, mass, and energy. The collision between such shells gives rise to internal shocks (reverse (RS) and forward (FS)), which convert the ordered bulk kinetic energy of the plasma into the magnetic field energy and the random kinetic energy of the particles. The highly accelerated particles then start to radiate and produce the emission observed from the jet. Here we apply the model of [2] to analyse the SEDs of OJ287, observed on 10/28/2008, and 3C279, observed on 01/15/2006 in its optical high state. We present the observed SEDs of 3C279 for a one month flaring period observed from 11/08/2008 - 12/08/2008 and quiescent period from 05/22/2010 - 05/22/2010 in order to gain insight on the evolution of its SEDs over longer time periods.

Internal Shock Model

The collision of two plasma shells results in an emission region as shown in Fig. 1. The treatment of shell collision and shock propagation is hydrodynamic and relativistic in nature [3].

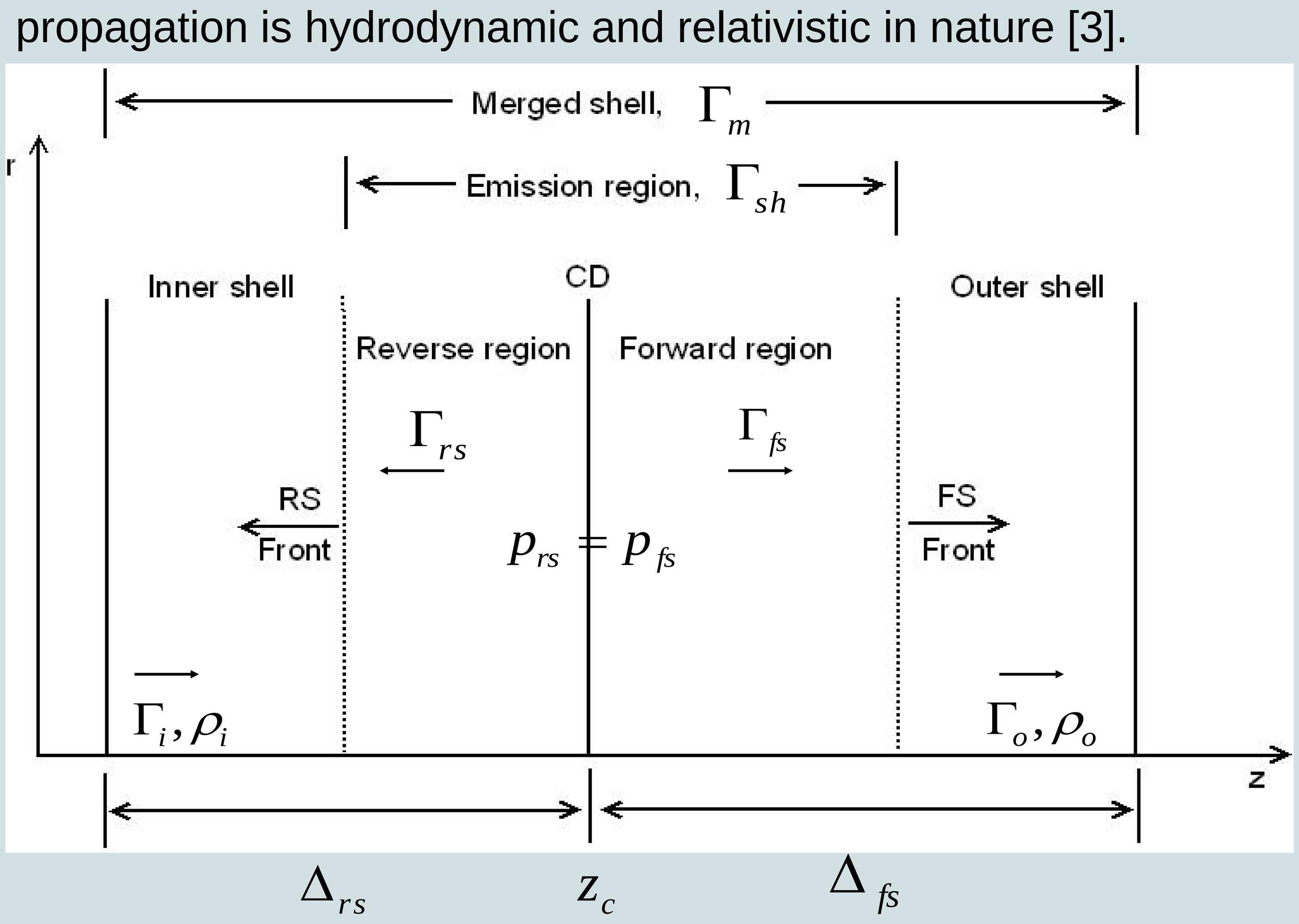

Fig. 1: Schematic of the emission region with RS traveling into the inner shell of BLF, Γ_i, and FS moving into the outer shell with BLF, Γ_o($\Gamma_i > \Gamma_o$). The pressures of the two shocked fluids, p_{rs} & p_{fs} are the same across the CD. Δ_{rs} & Δ_{fs} are the widths of the inner and outer shell after the collision in the lab frame (central engine frame) obtained from the shock dynamics [1].

Multi-slice Radiation Transfer Scheme

A cylindrical emission region has been considered to calculate the resultant spectrum in a time-dependent manner. The inhomogeneity in the photon and particle density throughout the emission region has been considered by dividing the region into multiple slices (Fig. 2) [2]. The radiation transfer (Eqn. 1 has been considered within each slice and in between the slices.

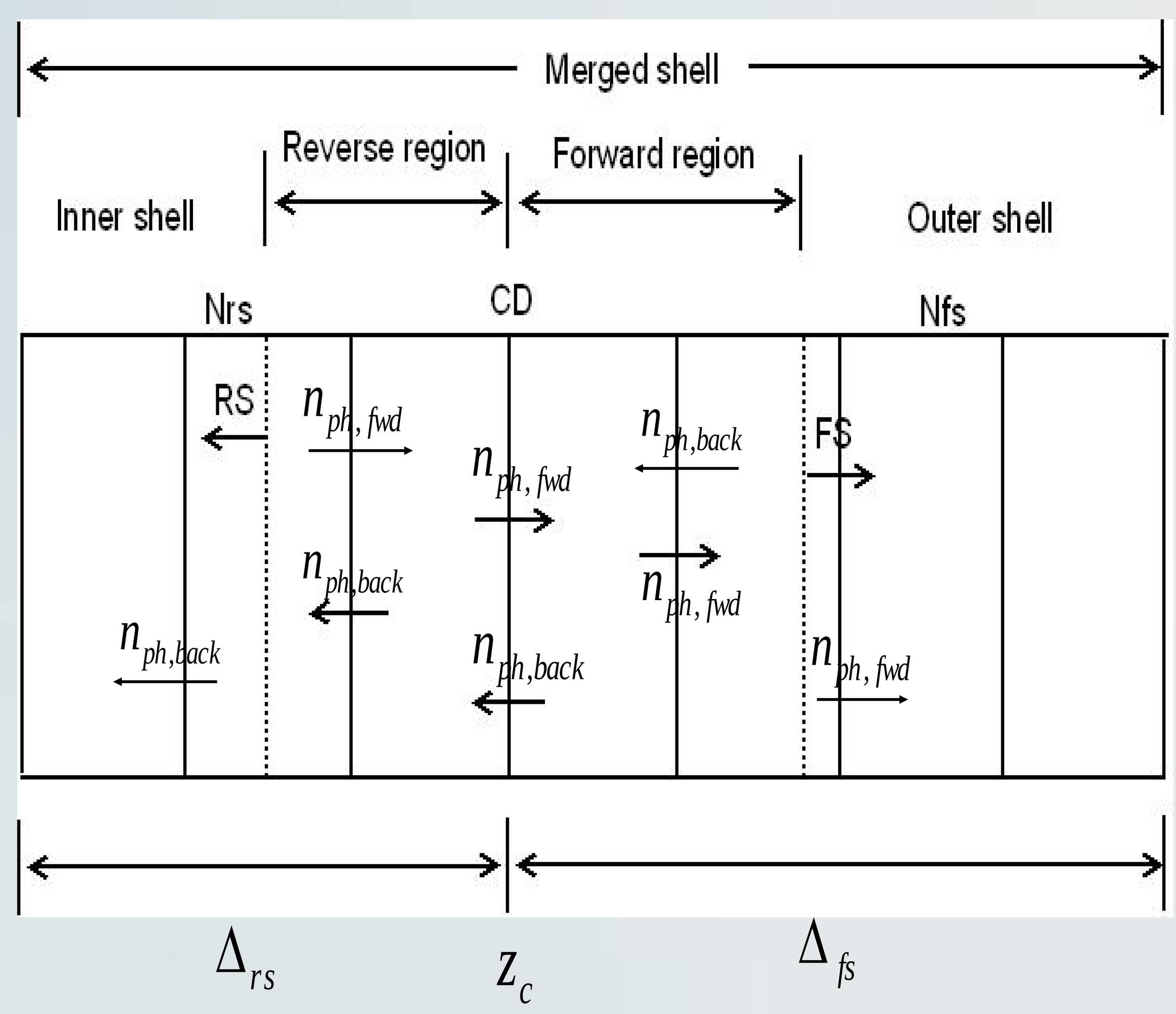

Fig. 2: Schematic of the radiation transfer in between the zones using appropriate photon escape probability functions.

$$dn_{ph,fwd} = n_{ph} \frac{dt}{t_{ph,esc}} P_{fwd} \qquad (1)$$

Future Development of Model

- •Include External Compton to reproduce observed SEDs.
- •Include inferred orientation of the magnetic field from polarization monitoring programs.
- •Study of intrinsic parameter differences between various blazar subclasses, arising from the orientation of the magnetic field in the jet.

First Results (Synchrotron + Synchrotron Self Compton):

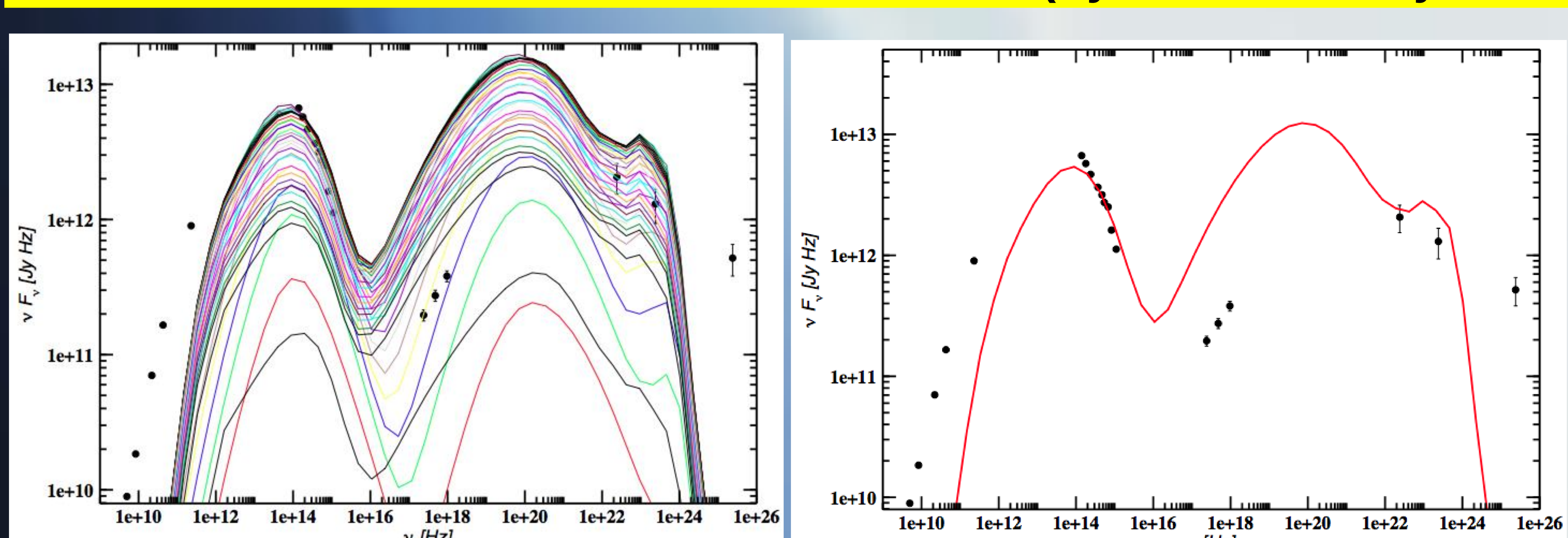

$L_{kin} \sim 2e48 ergs/s$

$R \sim 4e16; \Delta \sim 8e15 cm$

$\theta_{obs} \sim 2.5^\circ; q \sim 4.2$

$\Gamma_{sh} \sim 16.3$

$B \sim 2.5G$

$\gamma_{max} \sim 1e5$

$\gamma_{min,fs} \sim 6e2, \gamma_{min,rs} \sim 1e3$

Fig. 3: Simulated instantaneous and time-integraded (avergaed over 1.5 days) SED of OJ287 for 10/28/2008.

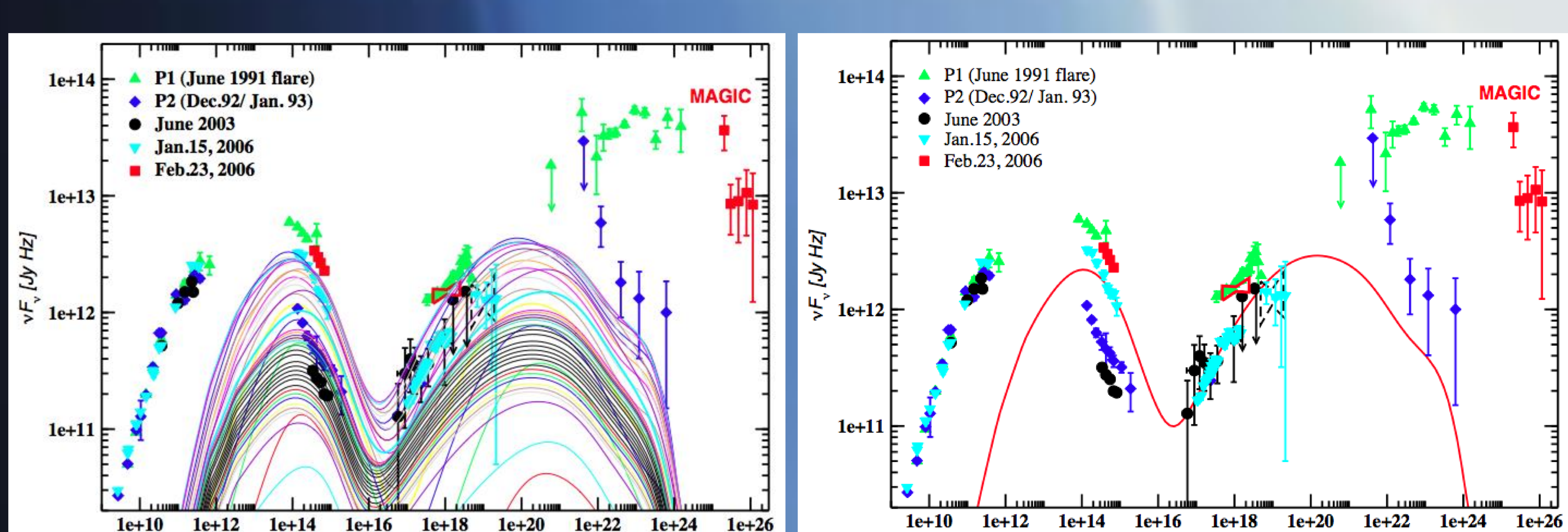

$L_{kin} \sim 1e48 ergs/s$

$R \sim 4e16; \Delta \sim 8e15 cm$

$\theta_{obs} \sim 2.5^\circ; q \sim 4.0$

$\Gamma_{sh} \sim 14.5$

$B \sim 2.8G$

$\gamma_{max} \sim 1e5$

$\gamma_{min,fs} \sim 8e2; \gamma_{min,rs} \sim 2e3$

Fig. 4: Simulated instantaneous and time-integrated (averaged over 1.5 days) SED 3C279 for 01/15/2006.

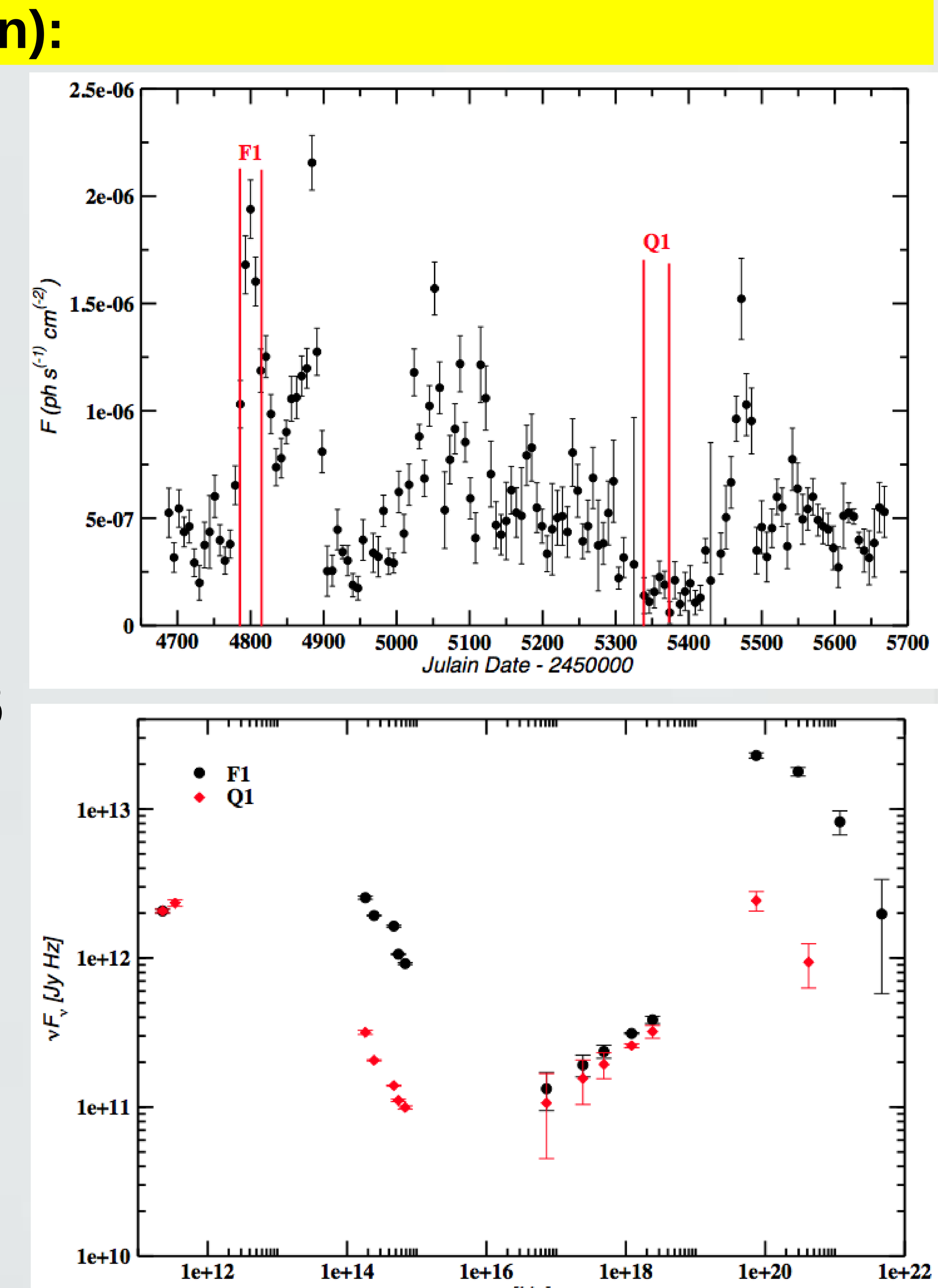

Fig. 5: Observed lightcurves from 08/09/2008 - 04/16/2011 and SED of 3C279 for periods F1 & Q1.

[1] Böttcher & Schlickeiser, R., 1997, A&A, 325, 866, [2] Joshi & Böttcher, 2011, ApJ, 727, 21, [3] Spada et al., 2001, MNRAS, 325, 1559

This research was supported in part by NASA through Fermi grants NNX10AO59G, NNX08AV65G, and NNX08AV61G and ADP grant NNX08AJ64G, and by NSF grant AST-0907893.